Geosci. Instrum. Method. Data Syst. Discuss., 2, 149–175, 2012
www.geosci-instrum-method-data-syst-discuss.net/2/149/2012/
doi:10.5194/gid-2-149-2012

Discussions Geoscientific Instrumentation Methods and Data Systems

Fractal analysis of INSAR and correlation with graph-cut based image registration for coastline deformation analysis: post seismic hazard assessment of the 2011 Tohoku earthquake region

P. K. Dutta[1] **and O. P. Mishra**[2,3]

[1]Advanced Digital Embedded System Lab, Electronics and Tele-Communication Dept., Jadavpur University, Kolkata, West Bengal 700041, India
[2]SAARC Disaster Management Centre (SDMC), IIPA Campus, Ring Road Delhi, Delhi 110002, India
[3]Geo-seismology Division, Geological Survey of India (CHQ), Kolkata, India

Received: 23 January 2012 – Accepted: 29 March 2012 – Published: 20 April 2012

Correspondence to: P. K. Dutta (ascendent1@gmail.com)

Published by Copernicus Publications on behalf of the European Geosciences Union.

Abstract

Satellite imagery for 2011 earthquake off the Pacific coast of Tohoku has provided an opportunity to conduct image transformation analyses by employing multi-temporal images retrieval techniques. In this study, we used a new image segmentation algorithm to image coastline deformation by adopting graph cut energy minimization framework. Comprehensive analysis of available INSAR images using coastline deformation analysis helped extract disaster information of the affected region of the 2011 Tohoku tsunamigenic earthquake source zone. We attempted to correlate fractal analysis of seismic clustering behavior with image processing analogies and our observations suggest that increase in fractal dimension distribution is associated with clustering of events that may determine the level of devastation of the region.

The implementation of graph cut based image registration technique helps us to detect the devastation across the coastline of Tohoku through change of intensity of pixels that carries out regional segmentation for the change in coastal boundary after the tsunami. The study applies transformation parameters on remotely sensed images by manually segmenting the image to recovering translation parameter from two images that differ by rotation. Based on the satellite image analysis through image segmentation, it is found that the area of 0.997 sq km for the Honshu region was a maximum damage zone localized in the coastal belt of NE Japan forearc region. The analysis helps infer using matlab that the proposed graph cut algorithm is robust and more accurate than other image registration methods. The analysis shows that the method can give a realistic estimate for recovered deformation fields in pixels corresponding to coastline change which may help formulate the strategy for assessment during post disaster need assessment scenario for the coastal belts associated with damages due to strong shaking and tsunamis in the world under disaster risk mitigation programs.

GID

2, 149–175, 2012

1 Introduction

The pacific coast of Tohuku in Northeast (NE) Japan has experienced past damaging inter-plate earthquakes due to heterogeneous rupture dimensions that overlap one after another (Nagai et al., 2001; Mishra et al., 2003). Studies by Mishra et al. (2003) revealed that the zone of the 2011 Tohoku tsunamigenic earthquake has a history of several past damaging scenario due to strong earthquake shakings and havoc tsunamis. Nagai et al. (2001) produced a comprehensive map of rupture distribution of past damaging earthquakes that showed overlaps of a mega-thrust earthquake of magnitude M_w 9.0 with the 1897 Miyagi-oki earthquake and the 1989 Sanriku earthquakes (M_w 7.5), in vicinity of which the 11 March 2011 tsunamigenic Tohoku earthquake rocked the coastal belt of NE Japan forearc region (Mishra et al., 2003; Mishra, 2004). The earthquake was located about 130 km east of the Sendai and about 430 km northeast of Tokyo (USGS, IRIS). The earthquake was so powerful that a killer tsunamis wave generated upto several meter heights that caused a huge devastation in the entire coastal belts of Miyagi, Fukusima and Sendai city of Northeast Japan. This is the greatest earthquake so far recorded in the history of Japan seismology. Maximum damage was reported by several agencies of Japan and overseas to show the damage in the coastal belt of NE Japan was mainly due to tsunamis and the subsequent fire that broke out due to strong shaking and tsunamis. There is a report on nuclear emission and leakage after the mega-thrust earthquake. This earthquake was associated with tremendously high seismic moment that was capable to displace the original location of the northeast part of the Honshu Island.

In order to quantify the precise deformation region, a homogenous field for analysis of devastation to surroundings is essential for monitoring an energy dissipation field which in this scenario is the satellite imagery. The robustness of the satellite images lies in the ability to be acquired globally in any time frame for feature based (Brown, 1992) and intensity based (Zitova and Flusser, 2003) analysis of the different segments in the image. Particularly, the physical identification of the changes involved for objects

GID
2, 149–175, 2012

– a task involving image segmentation analysis constitutes an essential issue for data analysis from satellite prospection. In fact, image segmentation can be understood as the process of assigning a label to every pixel in an image, the same label represent the same object. A graph cut image registraion technique has been proposed for extraction of damage region along the coastline and the results compared with fractal distribution models for damage information along the coastline of Tohoku. Automatic extraction of shoreline features from aerial photos has been investigated using neural nets and image processing techniques (Liu et al., 2011). The proposed study formulates a robust image information retrieval for the satellite imagery (Aubert and Kornprobst, 2006) to conform by delineating and labeling regions of interest (ROIs) on the reference image. The remotely sensed Advanced Synthetic Aperture Radar (ASAR) imagery acquired on 2 November 2010 as shown in Fig. 1a, representing the scenario of the coastal belt of Sendai prior to earthquake, while Fig. 1b showed the post tsunamigenic earthquake damage scenario of the region acquired on 21 March 2011. These images have been retrieved and diagnosed in the same visualization framework for change of pixel analysis for point by point correspondence mapping of disaster zones can be very useful to determine essential relations between the fractal value and damage level (Schubert et al., 2008). Analysis of the image transformation by non rigid registration schemes can detect the associated crustal deformation during the earthquake occurrence and termination phase (Thevenaz et al., 1998) presenting analysis of geometry of the ruptured fault and the energy released by the earthquake (Puymbroeck et al., 2000). The ASAR images are highly effective for large scale disaster analysis as it is free from climatic perturbations for any region unlike optical images from Advanced Space-borne Thermal Emission and Reflection Radiometer (ASTER) (Yamaguchi et al., 1998) sensors. ASAR imagery is applicable in remote sensing because of its robust applications having enhanced geometric correction accuracy.

The utilities of such studies in satellite image analysis for intensity and feature based extraction from remote sensing in multispectral classification are well documented in several fields, such as environmental monitoring studies, change detection

GID
2, 149–175, 2012

and weather forecasting (Radke et al., 2005; Holia and Thakar, 2009). The graph cut minimization framework as described in Boykov et al. (2001) is appropriately resolve detection of a phenomenon of a certain dimension, considering it as a registration problem. A formulation for region wise segmentation technique (Meng et al., 2011) in this framework may guide the minimization process towards a solution influenced externally. The outcome may provide collective information to a geo-analyst a scenario to utilize regional segmentation method for disaster analysis through remotely acquired satellite imagery for earthquake model. This approach can be used as a potential tool for post disaster loss assessment by policy makers, administrators, disaster managers to get a feedback for future investment purposes.

2 Methodology of pre-process and data retrieval

Most of the nature phenomena exhibit fractal characteristics (Sun et al., 2006; Chen and Chen, 1998), so fractal modeling of natural surfaces can play an important role in remote sensing for interpretation of surface physical phenomena. Image registration scheme has been analyzed by defining a motion for every pixel in the image. Data element set P representing the image pixels has a neighborhood for a set N representing all pairs $\{p,q\}$ of neighboring elements in P. In other words, the pixel sitting at a position $p(k)$ on the original image is known to have moved by $f(k)$ on the second image for a significant space window. If "A" be a vector specifying the assignment of pixel "p" in "P", then each "A_p" can be either in the background or the object. "A" defines a segmentation of "P", displacement label (vector) is assigned to each pixel in the source image to indicate the corresponding position in the floating image.

The image segmentation analysis in the proposed study has been categorically distributed into the following steps (a) preprocessing the satellite imagery for analysis, (b) image registration technique for minimization of mismatch between two images, (c) extraction of the optimal transformation from registration by calculating displacement of each pixel for energy minimization between two images, (d) regional

GID
2, 149–175, 2012

segmentation obtained from the various transformations produced by the different regions. Monitoring a process over a specific time or a long period needs a homogenous long data series statistical moments, can also be used to complement the characterization of the texture of geographical regions for spatial resolution analysis.

2.1 Image registration

An image registration technique developed here involves analysis of intensity of pixels extraction algorithm by precisely making a point to point correspondence for two (or more) images of the same area through geometrically aligning common features (or control points) identified in the images. Given a fixed image F as shown in Fig. 2a and a moving image M as shown in Fig. 2b, we show that non-parametric image registration may be treated as an optimization problem that aims at finding the displacement of each pixel for area of interest and decide if all pixels contained in the region satisfy some similarity constraint. The transformation models the spatial mapping of points from the fixed image space to the moving image space to analyze the deformation field of the pixels. The deformation field was evaluated for a pixel object representative energy function having two coefficients of a data dependent term and a smoothness term. Transformations for deformable surface to image registration provides better way to control the smoothness of the deformation field allowing a more complete framework for non-rigid registration with graph cut method. The image processing schemes involved in the process of deformable field extraction consists of feature detection, feature matching, transformation function estimation and image re-sampling. The transformation asserts the pixels in the moving image like a set of nodes, where each pixel move freely in a locally coherent connected to its neighbors by edges and Markov random field (MRF) pixel classification (Kato et al., 2001). After labeling the graph, a meaningful segmentation of the image from the deformation criterion (Miller et al., 1998) is obtained. The deformation field undergoes two forces, one that matches the moving image with the original image, the second that keeps the deformation field smooth. In order to register the original and moving images for point to point correspondence, we

GID
2, 149–175, 2012

need to optimize (Boykov et al., 2001b) over a given space of spatial transformations. Taking advantage of efficient algorithms for global min-cut solutions (Greig et al., 1989), were first to discover that powerful min-cut/max-flow algorithms from combinatorial optimization can be used to minimize certain important energy functions in visualization framework models. Centering that point, the displacement window obtained has been matched based on a threshold value for every pixel points with the same label share certain visual characteristics. Using the data analysis we have assigned various levels to the pixels and found the data cost term. This energy function gets optimized by graph cut (via alpha expansion) and optimum labeling is obtained.

2.2 Graph-cut based non-rigid registration and retrieving transformation

The graph cut method was introduced for interactive image segmentation that is unaffected by smoothness of the pixels flow but identify change of intensity associated with object boundaries. The study passes a new method to pass the deformation field across resolution levels in order to enable multi-level non-rigid registration using graph-cuts where P denote a set of pixels and segmentation can be done by assigning label $l_p \epsilon L$ to each pixel $p, q \epsilon P$, energy minimum function for pixel values resulting to

$$E(L) = \sum_{p \varepsilon P} D_p(l_p) + \sum_{(p,q) \varepsilon N} V_{p,q}(l_p, l_q) \quad (1)$$

The deformation field between two images I_1 and I_2 as source and moving image can be recovered by minimizing the energy as in Eq. (1). The first term, $D_p(l_p)$, measures how the data differs between the source image and the moving image. For instance, squared sum of differences as in Eq. (2) multimodal images (Lombaert et al., 2007) that implements mutual information can be used for analysis. The second term, $V_{p,q}(l_p, l_q)$ is an index of the smoothness coefficient for the deformation field. The technique involves constructing a specialized graph for the energy function to be minimized such that the minimum cut or maximum flow on the graph also minimizes the energy globally. According to the algorithm, on each pixel a velocity metric corresponding to crustal

GID
2, 149–175, 2012

deformation is defined with use of the intensity differences and gradient information. Let I and J respectively be the static image and the moving image of dimension d and $\boldsymbol{X}$ be the continuous spatial domain of both images. For any spatial point $x = (x_1, x_2 ... x_d) \in \boldsymbol{X}$, $I(\boldsymbol{x})$ and $J(\boldsymbol{x})$ are the intensity values (or feature vectors in general) at $\boldsymbol{x}$ of both images. In formulation, a transformation T represent a displacement vector field $\boldsymbol{D}$ which is relative to every point $\boldsymbol{x}$ displacement in J away from its original position by the vector $\boldsymbol{D}(\boldsymbol{x}) \in Rd$ to the new point $\boldsymbol{x} + \boldsymbol{D}(\boldsymbol{x})$. Optimize an assignment from a finite set of transformations through a discrete labeling problem.

$$\boldsymbol{D}^* = \text{argmin}\, C(I(\boldsymbol{X}), J(\boldsymbol{X} + \boldsymbol{D})) + \lambda S(\boldsymbol{D}). \tag{2}$$

The dissimilarity function C can be anything such as sum absolute difference (SAD), sum squared difference (SSD), normalized cross-correlation function or negative of the mutual information. Magnitude of the first derivative term as smoothness function S and get

$$\boldsymbol{D}^* = \text{argmin}\, C(I(\boldsymbol{X}), J(\boldsymbol{X} + \boldsymbol{D})) + \lambda \sum_{i=1}^{N} \int_X |\boldsymbol{D}xi| \mathrm{d}x \tag{3}$$

Where $\boldsymbol{D}(xi)$ is the first derivative of $\boldsymbol{D}$ along direction xi and the differential element $\mathrm{d}X = \mathrm{d}x_1 \mathrm{d}x_2 ... \mathrm{d}x$. $\mathrm{d}x + \boldsymbol{D}(\boldsymbol{x})$ in Eq. (3) can be any non-integer valued vector, and $J(\boldsymbol{x} + \boldsymbol{D}(\boldsymbol{x}))$ needs to be computed using an interpolation function. Also, when $\boldsymbol{x} + \boldsymbol{D}(\boldsymbol{x})$ is outside the image domain, a pre-assigned background intensity value can be used. Graph-cuts addresses segmentation in an optimization framework and finds a globally optimal solution for $\boldsymbol{D}^*$ in Eq. (3) for wide class of energy functions. The following phases apply in image registration using graph cut. Several speps are involved in the graph cut image transformation and registration, which are illustrated below:

1. A discrete labeling is applied to the deformed image $J(\boldsymbol{x} + \boldsymbol{D}(\boldsymbol{x}))$.
2. Feature matching is done to find transformations for moving parts of source to parts of target between the features in the reference and sensed image.

GID
2, 149–175, 2012

3. On feature matching, moved all the points as possibly close to the target by applying selected transformation $v = f_p(p)$.

4. Formulated energy function from these images $E = D+S$ where D is the data term and S is the smoothness term for the restriction imposed on the displacement of the neighboring pixels.

5. From similarity or dissimilarity measure assigned probable labels to the corresponding pixel.

6. Data term incorporated can be a similarity or dissimilarity measure between two images $I(\boldsymbol{x})$ and $J[\boldsymbol{x} + \boldsymbol{D}(\boldsymbol{x})]$ where $\boldsymbol{D}(\boldsymbol{x})$ is the deformation field and can be sum absolute difference. S term is for assigning markovianity among neighboring pixels represented by means based potts (Boykov et al., 1998) model having global smoothness term for preserving continuity.

7. Energy gets minimized for optimal image registration.

8. Retrieve transformation matrix from minimized energy function.

9. R is the distance within which the object k has a strong effect on point p. If the point p is at object of interest like shoreline, the λ assigned is infinity and it is not possible to assign the value $\boldsymbol{D}^*$ segment image and extracts the enclosed area, then determine the correct registration point.

10. Based on discrete labels, find the amount of transformation. The number of labels in each resolution is reduced and deformation vector field gets scaled to meet image resoultion in next finer level. Distance is used to measure alignment for a given label. Smoothness is used to restrict and clear different labels for adjacent cells.

11. Calculated area of difference transformation matrix for ranges.

GID
2, 149–175, 2012

12. Applied image translation for images through adjacency matrix.

13. Regional segmentation for transformation range of different pixels by using the search space to find the best alignment having intertwined components for pixel comparison and pixel grouping.

14. Calculated conditional entropy parameters of the images for local, joint and regional values has been calculated as in Table 3 that shows the disorder of the image.

15. Correlated with box counting method for fractal distribution estimation.

16. Relationship between fractal dimension and entropy features showed greater differences between the groups of pixels showing increase of entropy and fractal dimension for image after earthquake occurence.

We observed that the graph cuts introduce spatial domain information of the image that is lacking in the experimental results of the proposed method and compares the results with the single-level version demons (Thirion, 1998) method for non-parametric image registration for optimization finding the displacement of each pixel coherent and continually in spatial cluster regions that could be useful for cartographic classification (Boykov and Jolly, 2001). There are other segmentation algorithms in the literature which extends the concepts of graph cuts. Most prominent of them are graph cuts and lazy snapping (Li et al., 2004). Lazy snapping separates coarse and fine scale processing for making object specification and detailed adjustment easy in pixel separation. Beside, grab cuts (Rother et al., 2004) extends graph-cut by introducing iterative segmentation scheme to the image graph for refined segmentation schemes in intermediate steps. Segmentation with topology generation scenarios are set according to the resolution and scale of the expected objects. Clusters are extracted by traversing this tree and stopping nodes with distance smaller some threshold than certain threshold in region based extraction. By this method, not only single pixels are classified into refined clusters but also homogenous image objects are extracted during a previous

GID
2, 149–175, 2012

segmentation step. Grow cut (Vezhnevets and Konouchine, 2005) technique is given a small number of user-labeled pixels, the rest of the image is segmented automatically by a cellular automaton. The process is iterative, as the automaton labels the image, user can observe the segmentation evolution and guide the algorithm with human input where the segmentation is difficult to compute. In the areas, where the segmentation is reliably computed automatically no additional user effort is required.

3 Fractal analysis of damage

The fractal dimension is determined as the slope of the line which corresponds with the regional segmentation scenario. We attempted to assess damage through the fractal analyses of the data extracted from INSAR images acquired after earthquake. The box-counting method is found to be most appropriate approach for the purpose.

Suppose "*F*" is a limited fractal figure on a plane and when "*F*" is covered with square grids which are built by boxes whose side length is δ (A grid is namely a box), then the number of boxes intersecting on "*F*" is "*N*". If "*N*" is satisfied with the power law $N(\delta) \propto \delta - D$, then as $\delta \rightarrow 0$, the ratio of logarithm *FD* is estimated by means of the box-counting method (Ye and Chen, 2001).

In order to validate perspective distortion for the moving image (the image to segment), and the reference image, three phase optimization is implemented. The first phase involves recovering a non-rigid deformation field using graph cut with α epanision. The second shows how regional segmentation can influence the deformation map. The third is extraction of region based clusters through analysis of dissimilarity of pixel values implementing application of fractal techniques to image analysis. The proposed method is fast and robust against undesired change in imaging conditions. It was shown that the algorithm can be also efficiently used to detect damages caused by an earthquake. Images as shown in Fig. 2a, b correspond to two different captures of the same scene in different times rounded to 255 × 255 pixels. Region-based methodologies are predominant to segment the satellite image and active contour models are

GID
2, 149–175, 2012

preferred. A number of corresponding ground-control points from two images said the transformation parameters can be estimated for the images. The histogram of the image region was dissected into two parts using the global mean value as the dividing point. The mean and standard deviation were calculated for each image segmentation process as shown in Table 1. Clusters can then be extracted by traversing spatial locations for distance associated with smaller some threshold that can be visualized in extracting the coastline. Significance of the spatial location of coastline for analyzing refined region pixel shift analysis. The analysis shows logarithm linear relationship observed if their distribution in logarithm coordinate system tends to be linear as shown in Fig. 3 for the satellite imagery. The result shows that "Region A" has a relatively higher fractal dimension value compared with that of the "Region B", which is consistent with the analysis that the image in the post disaster zone had relatively higher number of small scale objects, causing relatively higher fractal dimension. Both regions also show difference from "Region C". The technique of manual image registration developed in this work is potentially powerful in terms of its registration accuracy as shown in Table 2, which demonstrates that the degree of automation, and its significant value in an operational context of homogenous regional classification are conspicuously possible from extracted data from satellite imagery. The matrix representation of the common spatial transformations (e.g. rigid body, affine, projective) in homogeneous coordinates can be well represented. The Euclidean representation is used to compute the spatial transformation (using e.g. matrix multiplication in homogeneous coordinates). This corresponds to optimum transformation and the resultant transformation of different pixels (voxels for 3-D) of the static image can be shown by the region based image segmentation algorithm. Based on the image mismatch, the projection of the relative displacement of each pixel in the two axes can be analyzed to evaluate the region where the maximum shift in the pixels takes place (Fig. 4). The maximum shift in the intensity of the pixels gives us an empirical measure of the area of maximum devastation which may be highly significant to conduct future remote sensing observation for a comprehensive analysis of geo-hazard distribution. From Table 2 it is evident that the

GID
2, 149–175, 2012

pixel wise displacement values for intensity based registration of images is discretized in different ranges such as 0–10, 10–20, 20–30, 30–40 in different columns as shown in Fig. 5, which is regionally extracted from the moving image.

The region extraction through regional segmentation analysis for the nature of devastation reveals from Table 2, suggesting that 1031 pixels for the region of maximum devastation has suffered the maximum displacement in terms of change in the number of pixels. The region of maximum devastation is evaluated by multiplying the cluster of pixels for region with the spatial resolution of each pixel corresponding to appoint in the satellite imagery for estimation of the area of devastation. In this image, the spatial resolution of the Envisat image is 30 m equivalent to a pixel which means one single pixel refers to the area of 30^2 or 900 squares of meters. After the multiplication of pixel change based on intensity and resolution, $1031 \times 30^2\ m^2 = 0.9279 \times 10^6\ m^2$ corresponding to 0.997 sq km is the region that has undergone the maximum devastation. This image is divided into 4 – sub-images and numbered in turn as A, B, C and D. These are judge for non-zero sub-matrixes. Our analyses suggest that the 4 sub-images, A, B and C and D have clear linear tendency (Figs. 5–6), indicating that the considered devastated area has the characteristic of a fractal. Using the least square method these points are fit into a line.

4 Conclusions

This article implements the graph cut-α expansion that enables usage of a concurrent segmentation and registration as mutually supporting processes for region based cluster mapping. The graph cut analysis provides vivid outlook into the boundary and regional penalty model to achieve more accurate results for remote analysis of the imagery data. Comprehensive analysis of available INSAR images using coastline deformation analysis helped extract disaster information of the affected region of the 2011 Tohoku tsunamigenic earthquake source zone. We attempted to correlate fractal analysis of seismic clustering behavior with image processing analogies and our observation

GID
2, 149–175, 2012

suggests that increase in fractal dimension distribution is associated with clustering of events that may determine the level of devastation of the region. The results have been compared with fractal dimension analysis that shows that fractal dimension distribution coefficient increases pixel changes as identified from Fig. 6. Extensive visual comparison shows that the relative accuracy of the resultant coastlines within one image pixel compared with the human visual interpretation of the features. The results give conclusive evidence that fractal techniques can be extensively used for identifying the various features present in a satellite INSAR image. Box counting method is very effective for deriving the fractal dimensions. The future work will involve analyzing precursory data models with damaged distribution area extracting shape priors from existing data, and use this information to find analogy between seismic clusters and segmented regions for similar pattern recognition to produce a stable and physically consistent seismic cluster in any region of moderate seismicity.

Based on the satellite image analysis through image segmentation, it is found that the area of 997 km^2 for the Honshu region was a maximum damage zone localized in the coastal belt of NE Japan forearc region. The analysis helps infer using matlab that the proposed graph cut algorithm is robust and more accurate than other image registration methods. The analysis shows that the method can give a realistic estimation for recovered deformation fields in pixels corresponding to coastline change which may help formulate strategy for the post disaster need assessment of the region associated with strong shaking and tsunamis for disaster risk mitigation programs for the region of analogous disaster scenario. The outcome of this study may provide collective information to a geo-analyst to utilize regional segmentation method for disaster analysis through remotely acquired satellite imagery for earthquake model. This approach can be used as a potential tool for post disaster loss assessment by policy makers, administrators, disaster managers to get a feedback for development of strategy for future investment in the disaster prone regions of the world.

Acknowledgements. Authors express gratitude to the European Space Agency for providing Images of the 2011 Tsunamigenic Tohoku earthquake (M_w 9.0) of both pre- and post-disaster

GID
2, 149–175, 2012

scenarios. P. K. D. expresses thanks to M. K. Naskar, University of Jadavpur for his encouragement and motivation to take up study under O. P. Mishra, Seismologist having pioneering researches in the NE Japan forearc region and elsewhere in the world.

References

Aubert, G. and Kornprobst, P.: Mathematical problems in image processing: Partial Differential Equations and the Calculus of Variations, Springer, Applied Mathematical Sciences, 147, 377 pp., 2006.

Brown, L.: A survey of image registration techniques, ACM Computing Surveys, 24, 325–376, doi:10.1145/146370.146374, 1992.

Boykov, Y. and Jolly, M. P.: Interactive Graph Cuts for Optimal Boundary & Region Segmentation of Objects in N-d Images, in: International Conference on Computer Vision, (ICCV), I, 105–112, 2001.

Boykov, Y., Veksler, O., and Zabih, R.: Markov random fields with efficient approximations, in: IEEE Conference on Computer Vision and Pattern Recognition, 33, 648–655, doi:10.1109/CVPR.1998.698673, 1998.

Boykov, Y., Lee, V. S., Rusinek, H., and Bansal, R.: Segmentation of dynamic N-D data sets via graph cuts using markov models, in: Medical Image Computing and Computer-Assisted Intervention (MICCAI), 1058–1066, 2001a.

Boykov, Y., Veksler, O., and Zabih, R.: Fast approximate energy minimization via graph cuts, in: IEEE Transactions on Pattern Analysis and Machine Intelligence, 23, 1222–1239, 2001b.

Chen, Y. and Chen, L.: The fractal geometry, Beijing: Earthquake Publishing, 1998.

European Space Agency: ESA Earth Watching, 2011.

Greig, D., Porteous, B., and Seheult, A.: Exact maximum a posteriori estimation for binary images, J. Roy. Stat. Soc. B, 51, 271–279, 1989.

Holia, M. and Thakar, V. K.: Image registration for recovering affine transformation using Nelder Mead Simplex method for optimization, avalaible at: http://www.cscjournals.org/csc/manuscript/Journals/IJIP/volume3/Issue5/IJIP-76.pdf, 2009.

Kato, Z., Pong, T. C., and Chung-Mong, L.: Color image segmentation and parameter estimation in a Markovian framework, Pattern Recogn. Lett., 22, 309–321, 2001.

GID

2, 149–175, 2012

Kraft, R.: Fractals and Dimensions, http://web2.wzw.tum.de/ane/dimensions/dimensions.html, 1995.
Li, Y., Sun, J., Tang, C. K., and Shum, H. Y.: Lazy Snapping, in: Proceedings of ACMSIGGRAPH, 303–308, 2004.
Liu, H., Wang, L., Sherman, D. J., Wu, Q., and Su, H.: Algorithmic Foundation and Software Tools for Extracting Shoreline Features from Remote Sensing Imagery and LiDAR Data, Journal of Geographic Information System, 3, 99–119, doi:10.4236/jgis.2011.32007, 2011.
Lombaert, H., Sun, Y., and Cheriet, F.: Landmark-Based Non-rigid Registration Via Graph Cuts, in: Proc. of the 4th International Conference, ICIAR 2007, LNCS, 4633, 166–175, 2007.
Meng, Li, Chuanjiang He and Yi Zhan: Adaptive level-set evolution without initial contours for image segmentation, J. Electron. Imaging, 20, 023004, doi:10.1117/1.3574770, 2011.
Miller, M. I., Joshi, S. C., and Christensen, G. E.: Large deformation fluid diffeomorphisms for landmark and image matching, in: Toga, A., edited by: Warping, B., 1998.
Mishra, O. P.: Lithospheric heterogeneities and seismotectonics of NE Japan forearc and Indian regions, D.Sc. thesis, GRC, Ehime University, Japan, 223 pp., 2004.
Mishra, O. P., Zhao, D., Umino, N., and Hasegawa, A.: Tomography of northeast Japan forearc and its implications for interplate seismic coupling, Geophys. Res. Lett., 30, 1850, doi:10.1029/2003GL017736, 2003.
Nagai, R., Kikuchi, M., and Yamanaka, Y.: Comparative study on the source process of recurrent large earthquakes in Sanriku-oki Region: The 1968 Tokachi-oki earthquake and the 1994 Sanriku-oki earthquake, Zisin, 54, 267–280, 2001 (in Japanese with English abstract).
Puymbroeck, N. V., Michel, R., Binet, R., Avouac, J. P., and Taboury, J.: Measuring Earthquakes from Optical Satellite Images, Appl. Optics, 39, 3486–3494, 2000.
Radke, R. J., Andra, S., Al-Kofahi, O., and Roysam, B.: Image change detection algorithms: a systematic survey, in: Image Processing, IEEE T. Signal. Proces., 14, 294–307, doi:10.1109/TIP.2004.838698, 2005.
Rother, C., Blake, A., and Kolmogorov, V.: Graphcut – Interactive Foreground Extraction Using Iterated Graph Cuts, in: Proceedings of SIGGRAPH, 309–314, doi:10.1145/1015706.1015720, 2004.
Schubert, A., Small, D., Miranda, N., and Meier, E.: ASAR Product Consistency and Geolocation Accuracy, in: Proceedings of the CEOS SAR Cal/Val Workshop, Oberpfaffenhofen, Germany, November 2008.

GID
2, 149–175, 2012

Sun, W., Xu, G., Gong, P., and Liang, S.: Fractal Analysis of Remotely Sensed Images: A review of methods and applications, Review Article, Int. J. Remote Sens., 27, 4963–4990, 2006.
US Geological Survey, Earthquake Hazards Program: http://earthquake.usgs.gov/earthquakes/recenteqsww/, last access: 27 October 2011.
Thirion, J.: Image matching as a diffusion process: an analogy with maxwell's demons, MedIA, 2, 243–260, 1998.
Thevenaz, P., Ruttimann, U. E., and Unser, M.: A pyramidal approach to subpixel registration based on intensity, in: IEEE Trans. on Image Processing, 7, 27–41, doi:10.1109/83.650848, 1998.
Vezhnevets, V. and Konouchine, V.: GrowCut: Interactive multi-label N-D image segmentation by cellular automata, Proc. of Graphicon, 150–156, 2005.
Yamaguchi, Y., Kahle, A. B., Tsu, H., Kawakami, T., and Pniel, M.: Overview of Advanced Spaceborne Thermal Emission and Reflectance Radiometer (ASTER), IEEE T. Geosci. Remote Sens., 36, 1062–1071, doi:10.1109/36.700991, 1998.
Ye, J. and Chen, B. Z.: The application of the fractal theory in the city research, Urban Planning Forum, 4, 38–42, 2001.
Zitova, B. and Flusser, J.: Image registration methods: a survey, Image Vision Comput., 21, 977–1000, doi:10.1016/S0262-8856(03)00137-9, 2003.

GID
2, 149–175, 2012

Table 1. Absolute Intensity Difference for statistical emissivity values (the mean, the standard deviation) for comparative measure of accuracy of regional segmentation values.

Registration Algorithm	Mean	Standard Deviation
Demons Algorithm	12.6100	27.1190
Graph Cut-α expansion	0.2449	4.4666
Graph cut-lazy snapping	0.2889	5.332

GID
2, 149–175, 2012

Table 2. First five normalized joint intensity histogram analysis at 4 different locations.

Region displacement classification	Pixelwise displacement
0–10	5.2×10^4
10–20	0.93×10^4
20–30	5831
30–40	1031
40–50	890

GID
2, 149–175, 2012

Table 3. Maximum Entropy extracted from satellite images on the threshold based on regional segmentation.

Acquired Image	Local Entropy	Joint entropy	Global Relative Entropy
Before earthquake Image	140	36	145
After Earthquake Image	122	16	127

GID
2, 149–175, 2012

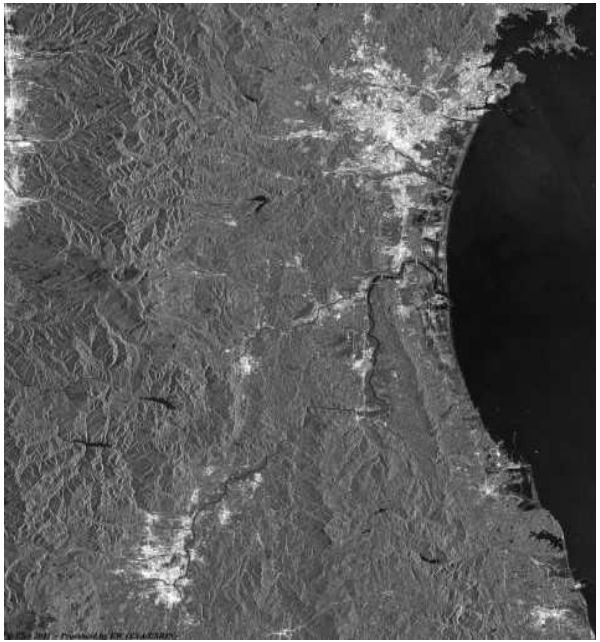

Fig. 1a. Acquired ASAR Image on 21 November 2010 before the earthquake/tsunami from Envisat satellite.

GID
2, 149–175, 2012

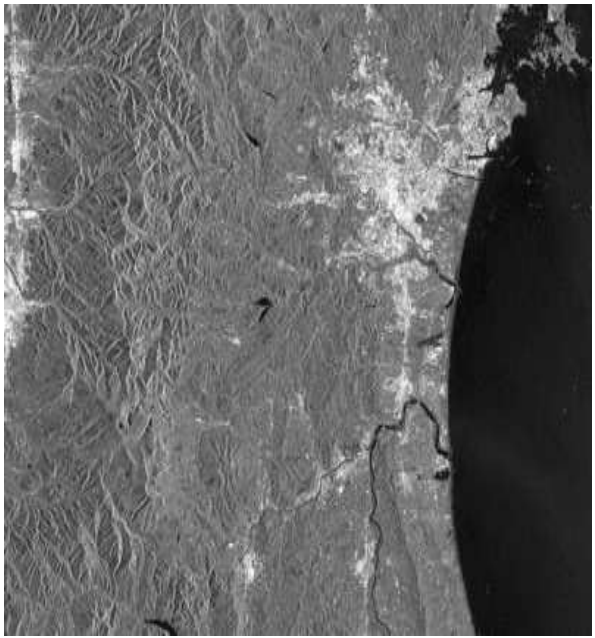

Fig. 1b. Acquired ASAR image on 21 March 2011 after the earthquake from Envisat satellite.

GID
2, 149–175, 2012

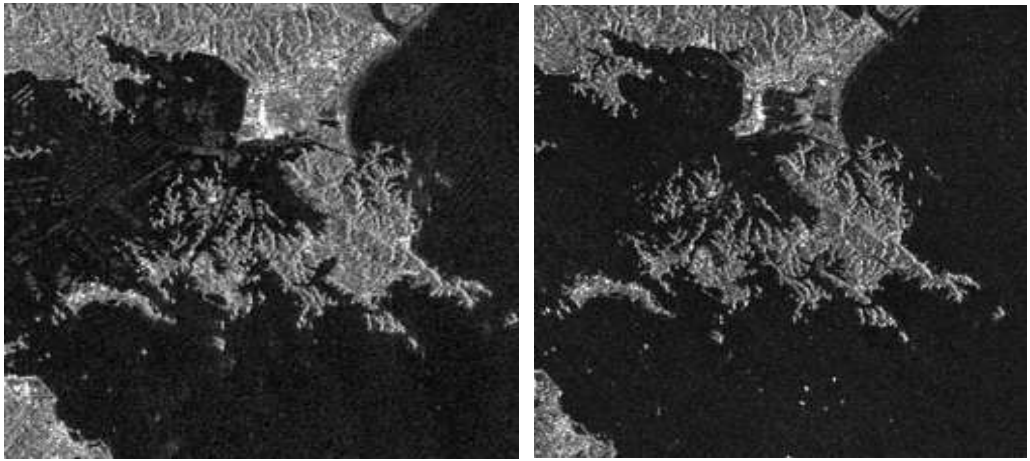

Fig. 2. (a, b) Emissivity images (RGB = Band 14, 12, 10) retrieved from Static image (before earthquake) on the left and for Moving Image (after earthquake).

GID
2, 149–175, 2012

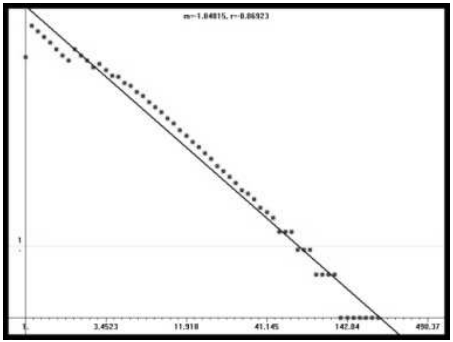

RegionA(D=1.85)

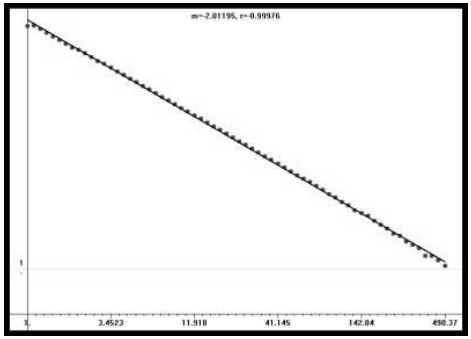

RegionB(D=2.01)

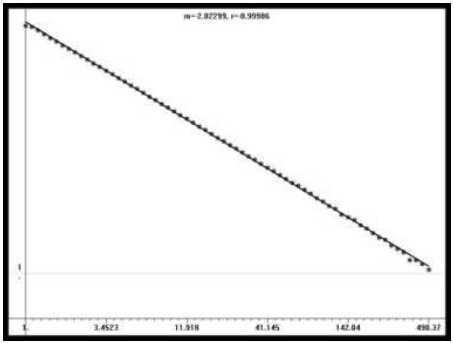

RegionC(D=2.02)

Fig. 3. The INSAR images (up) and dimensions (down) of different regions in imagery acquired from Tohuku.

GID
2, 149–175, 2012

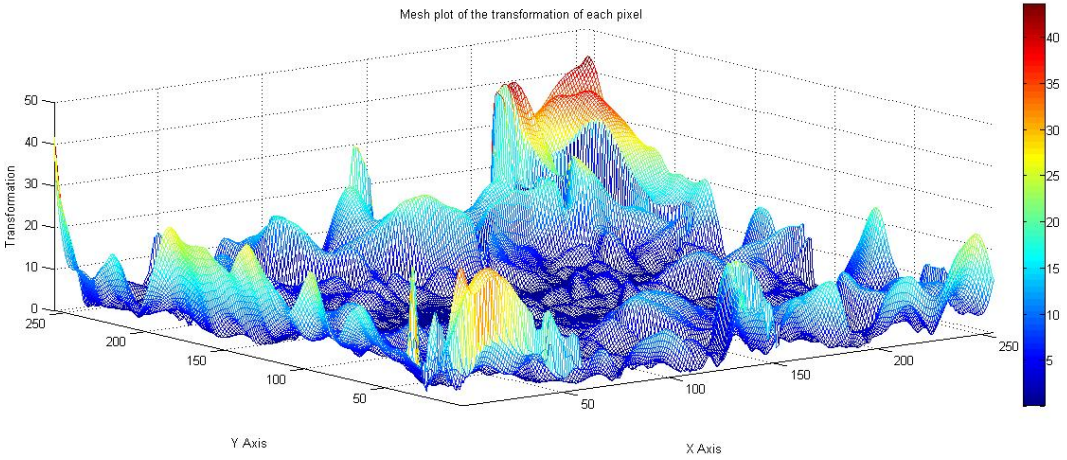

Fig. 4. Plot of transformation of different pixels of static image.

GID
2, 149–175, 2012

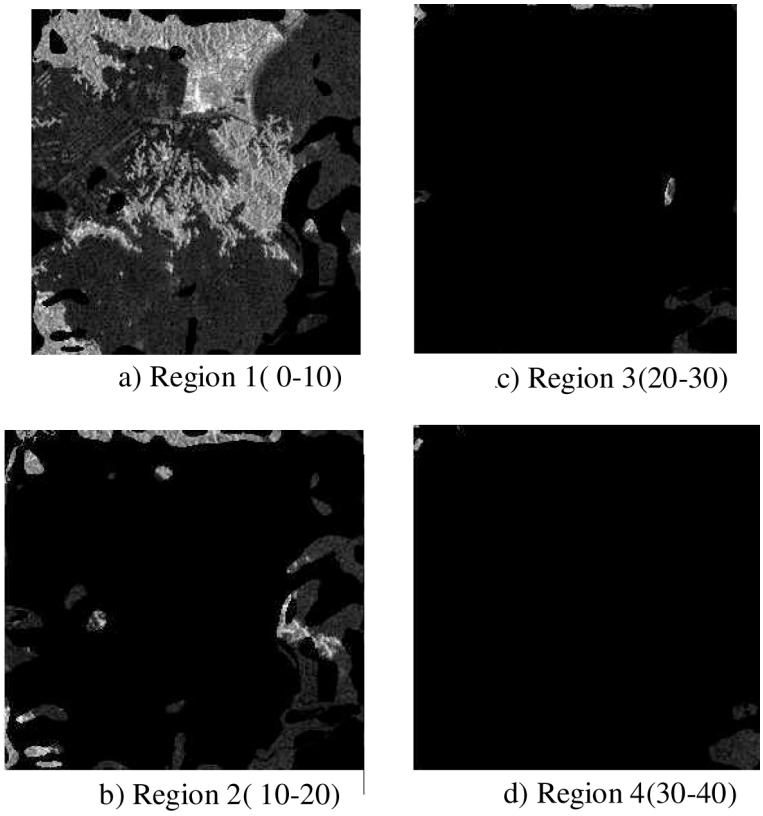

Fig. 5. Manual Segmentation for each region for displacement **(a, b, c, d)** of the pixels.

GID
2, 149–175, 2012

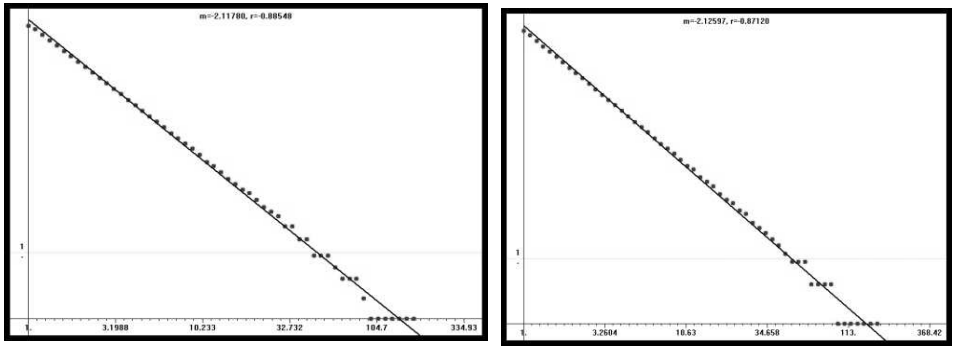

Region A:2.01 Region B:2.03

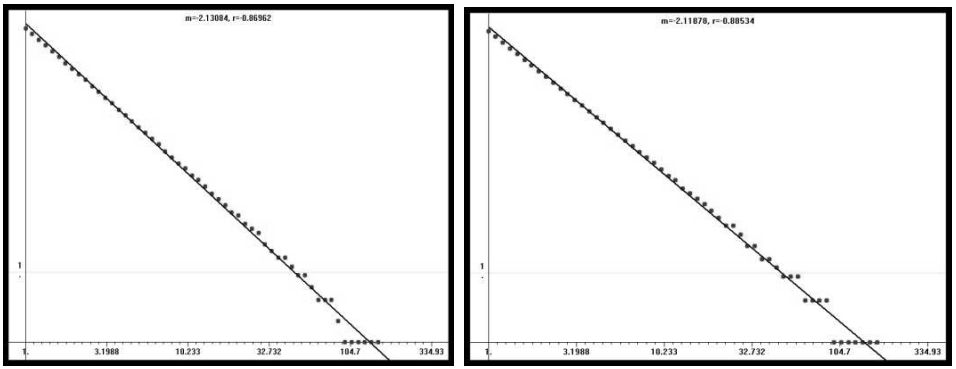

Region C:2.04 Region D:2.12

Fig. 6. Fractal Dimension estimation of each region from Fig. 5.

GID
2, 149–175, 2012